Transcriptomic response of *Nitrosomonas europaea* transitioned from ammonia- to oxygen-limited steady-state growth

Christopher J. Sedlacek[1,2*,#], Andrew T. Giguere[1,3,7*], Michael D. Dobie[4], Brett L. Mellbye[4], Rebecca V Ferrell[5], Dagmar Woebken[1], Luis A. Sayavedra-Soto[6], Peter J. Bottomley[3,4], Holger Daims[1,2], Michael Wagner[1,2,7], Petra Pjevac[1,8]

[1]University of Vienna, Centre for Microbiology and Environmental Systems Science, Division of Microbial Ecology, Vienna, 1090, Austria.

[2]University of Vienna, The Comammox Research Platform, Vienna, 1090 Austria.

[3]Department of Crop and Soil Science, Oregon State University, Corvallis, OR, 97331, USA.

[4]Department of Microbiology, Oregon State University, Corvallis, OR, 97331, USA.

[5]Department of Biology, Metropolitan State University of Denver, Denver, CO 80217, USA

[6]Department of Botany and Plant Pathology, Oregon State University, Corvallis, OR, 97331, USA

[7]Center for Microbial Communities, Department of Chemistry and Bioscience, Aalborg University, Denmark

[8]Joint Microbiome Facility of the Medical University of Vienna and the University of Vienna, Vienna, Austria

Keywords:

Transcriptome, ammonia and oxygen limitation, chemostat, ammonia-oxidizing bacteria, *Nitrosomonas europaea*

*These authors contributed equally

Running Title: Oxygen-limited growth of *Nitrosomonas europaea*

Address correspondence to:
Chris Sedlacek
University of Vienna
Althstrasse 14
1090 Vienna,
Austria
Email: sedlacek@microbial-ecology.net
Phone: +43 1 4277 91237

Abstract word count: 250

Text word count: 4885

Abstract

Ammonia-oxidizing microorganisms perform the first step of nitrification, the oxidation of ammonia to nitrite. The bacterium *Nitrosomonas europaea* is the best characterized ammonia oxidizer to date. Exposure to hypoxic conditions has a profound effect on the physiology of *N. europaea*, e.g. by inducing nitrifier denitrification, resulting in increased nitric and nitrous oxide production. This metabolic shift is of major significance in agricultural soils, as it contributes to fertilizer loss and global climate change. Previous studies investigating the effect of oxygen limitation on *N. europaea* have focused on the transcriptional regulation of genes involved in nitrification and nitrifier denitrification. Here, we combine steady-state cultivation with whole genome transcriptomics to investigate the overall effect of oxygen limitation on *N. europaea*. Under oxygen-limited conditions, growth yield was reduced and ammonia to nitrite conversion was not stoichiometric, suggesting the production of nitrogenous gases. However, the transcription of the principal nitric oxide reductase (cNOR) did not change significantly during oxygen-limited growth, while the transcription of the nitrite reductase-encoding gene (*nirK*) was significantly lower. In contrast, both heme-copper containing cytochrome *c* oxidases encoded by *N. europaea* were upregulated during oxygen-limited growth. Particularly striking was the significant increase in transcription of the B-type heme-copper oxidase, proposed to function as a nitric oxide reductase (sNOR) in ammonia-oxidizing bacteria. In the context of previous physiological studies, as well as the evolutionary placement of *N. europaea's* sNOR with regards to other heme-copper oxidases, these results suggest sNOR may function as a high-affinity terminal oxidase in *N. europaea* and other AOB.

57 **Importance**

58 Nitrification is a ubiquitous, microbially mediated process in the environment and an essential
59 process in engineered systems such as wastewater and drinking water treatment plants. However,
60 nitrification also contributes to fertilizer loss from agricultural environments increasing the eutrophication
61 of downstream aquatic ecosystems and produces the greenhouse gas nitrous oxide. As ammonia-
62 oxidizing bacteria are the most dominant ammonia-oxidizing microbes in fertilized agricultural soils,
63 understanding their response to a variety of environmental conditions is essential for curbing the
64 negative environmental effects of nitrification. Notably, oxygen limitation has been reported to
65 significantly increase nitric oxide and nitrous oxide production during nitrification. Here we investigate the
66 physiology of the best characterized ammonia-oxidizing bacterium, *Nitrosomonas europaea,* growing
67 under oxygen-limited conditions.

1 Introduction

Nitrification is a microbially mediated, aerobic process involving the successive oxidation of ammonia (NH_3) and nitrite (NO_2^-) to nitrate (NO_3^-) (1). In oxic environments, complete nitrification is accomplished through the complimentary metabolisms of ammonia-oxidizing bacteria (AOB) / archaea (AOA) and nitrite-oxidizing bacteria (NOB), or by comammox bacteria (2, 3). The existence of nitrite-oxidizing archaea (NOA) has been proposed, but not yet confirmed (4). Although an essential process during wastewater and drinking water treatment, nitrification is also a major cause of nitrogen (N) loss from N amended soils. Nitrifiers increase N loss through the production of NO_3^-, which is more susceptible to leaching from soils than ammonium (NH_4^+), serves as terminal electron acceptor for denitrifiers, and contributes to the eutrophication of downstream aquatic environments (5).

In addition, ammonia oxidizers produce and release nitrogenous gases such as nitric (NO) and nitrous (N_2O) oxide during NH_3 oxidation at a wide range of substrate and oxygen (O_2) concentrations (6, 7). Nitrogenous gases are formed through enzymatic processes (8-13), but also by a multitude of chemical reactions that use the key metabolites of ammonia oxidizers, hydroxylamine (NH_2OH) and NO_2^- (or its acidic form HNO_2), as the main precursors (14, 15). AOB, in particular, release NO and N_2O either during NH_2OH oxidation (16-21) or via nitrifier denitrification - the reduction of NO_2^- to N_2O via NO (22-25). The first pathway is the dominant process at atmospheric O_2 levels, while the latter is more important under O_2-limited (hypoxic) conditions (26, 27), where NO_2^- and NO serve as alternative sinks for electrons generated by NH_3 oxidation.

Nitrosomonas europaea strain ATCC 19718 was the first AOB to have its genome sequenced (28), and is widely used as a model organism in physiological studies of NH_3 oxidation and NO/N_2O production in AOB (27, 29-36). The enzymatic background of NO and N_2O production in *N. europaea* is complex and involves multiple interconnected processes (Fig. 1). Most AOB encode a copper-containing nitrite reductase, NirK, which is necessary for efficient NH_3 oxidation by *N. europaea* at atmospheric O_2 levels. NirK is also involved in but not essential for NO production during nitrifier denitrification in *N. europaea* (26, 27, 29, 35), and is upregulated in response to high NO_2^- concentrations (37). Moreover, two forms of membrane-bound cytochrome (cyt) *c* oxidases (cNOR and sNOR), and three cytochromes

95 referred to as cyt P460 (CytL), cyt *c'* beta (CytS) and cyt c_{554} (CycA), have been implicated in N_2O
96 production in *N. europaea* and other AOB (12, 24, 32, 38-40). However, the involvement of cyt c_{554} in
97 N_2O production has recently been disputed (41). Finally, recent research has confirmed that the
98 oxidation of NH_3 to NO_2^- in AOB includes the formation of NO as an obligate intermediate, produced by
99 NH_2OH oxidation via the hydroxylamine dehydrogenase (HAO) (20). The enzyme responsible for the
100 oxidation of NO to NO_2^- (the proposed nitric oxide oxidase) has not yet been identified (40).

101 The production of NO and N_2O by *N. europaea*, grown under oxic as well as hypoxic conditions,
102 has been previously demonstrated and quantified in multiple batch and chemostat culture studies (11,
103 12, 34, 35, 42, 43). Furthermore, recent studies have investigated the instantaneous rate of NO and N_2O
104 production by *N. europaea* during the transition from oxic to hypoxic or anoxic conditions (12, 35, 36).
105 Despite this large body of literature describing the effect of oxygen (O_2) limitation on NH_3 oxidation and
106 NO/N_2O production in *N. europaea*, little attention has been paid to the regulation of other processes
107 under these conditions. Previous studies have utilized reverse transcription quantitative polymerase
108 chain reaction (RT-qPCR) assays to examine transcriptional patterns of specific, mainly N-cycle related
109 genes in AOB grown under O_2-limited conditions (34, 36, 44). To date, no study has evaluated the global
110 transcriptomic response of *N. europaea* to O_2-limited growth. However, research on the effect of
111 stressors other than reduced O_2 tension have demonstrated the suitability of transcriptomics for the
112 analysis of physiological responses in AOB (43, 45-48).

113 *N. europaea* utilizes the Calvin-Benson-Bassham (CBB) cycle to fix inorganic carbon (28, 49).
114 Whereas all genome-sequenced AOB appear to use the CBB cycle, differences exist in the number of
115 copies of ribulose-1,5-bisphosphate carboxylase/oxygenase (RuBisCO) genes encoded, as well as the
116 presence or absence of carbon dioxide (CO_2) concentrating mechanisms (50-52). *N. europaea* encodes
117 a single Form IA green-like (high affinity) RuBisCO enzyme and two carbonic anhydrases, but no
118 carboxysome related genes (28). RuBisCO is considered to function optimally in hypoxic environments,
119 as it also uses O_2 as a substrate and produces the off-path intermediate 2-phosphoglycolate (53, 54).
120 However, the effect of O_2 limitation on the transcription of RuBisCO encoding genes and resulting growth
121 yield in AOB is still poorly understood.

In this study, we expand upon previous work investigating the effects of O_2 limitation on *N. europaea*, by profiling the transcriptomic response to substrate (NH_3) versus O_2 limitation. *N. europaea* was grown under steady-state NH_3- or O_2-limited conditions, which allowed for the investigation of differences in transcriptional patterns between growth conditions. We observed a downregulation of genes associated with CO_2 fixation, as well as increased expression of two distinct heme-copper containing cytochrome *c* oxidases (HCOs) during O_2-limited growth. Our results provide new insights into how *N. europaea* physiologically adapts to thrive in O_2-limited environments, and identified putative key enzymes for future biochemical characterization.

2 Materials and Methods

2.1 Cultivation

N. europaea ATCC 19718 was cultivated at 30°C, as a batch and continuous chemostat culture as previously described (43, 48). Briefly, *N. europaea* was grown in mineral media containing 30 mmol L^{-1} $(NH_4)_2SO_4$, 0.75 mmol L^{-1} $MgSO_4$, 0.1 mmol L^{-1} $CaCl_2$, and trace minerals (10 µmol L^{-1} $FeCl_3$, 1.0 µmol L^{-1} $CuSO_4$, 0.6 µmol L^{-1} $Na_2Mo_4O_4$, 1.59 µmol L^{-1} $MnCl_2$, 0.6 µmol L^{-1} $CoCl_2$, 0.096 µmol L^{-1} $ZnCl_2$). After sterilization by autoclaving, the media was buffered by the addition of 6 mL L^{-1} autoclaved phosphate-carbonate buffer solution (0.52 mmol L^{-1} NaH_2PO_4 x H_2O, 3.5 mmol L^{-1} KH_2PO_4, 0.28 mmol L^{-1} Na_2CO_3, pH adjusted to 7.0 with HCl).

For steady-state growth, a flow through bioreactor (Applikon Biotechnology) with a 1 L working volume was inoculated with 2% (v/v) of an exponential phase *N. europaea* batch culture. The bioreactor was set to 'batch' mode until the NH_4^+ concentration reached <5 mmol L^{-1} (six days; Table S1). Subsequently, the bioreactor was switched to continuous flow 'chemostat' mode, at a dilution rate / specific growth rate (µ) of 0.01 h^{-1} (doubling time = ~70 hours), which was controlled by a peristaltic pump (Thermo Scientific). The culture was continuously stirred at 400 rpm and the pH was automatically maintained at 7.0 ± 0.1 by addition of sterile 0.94 mol L^{-1} (10% w/v) Na_2CO_3 solution. Sterile filtered (0.2 µm) air, at a rate of 40 ml min^{-1}, was supplied during batch and NH_3-limited steady-state growth. Once

148 NH_3-limited steady-state was reached (day 7), the chemostat was continuously operated under NH_3-
149 limited conditions for 10 days. To transition to O_2-limited steady-state growth, after day 16, the air input
150 was stopped and the stirring speed was increased to 800 rpm to facilitate gas exchange between the
151 medium and the headspace. O_2-limited steady-state growth was achieved on day 23 as defined by the
152 persistence of 26.4 - 31 mmol L^{-1} NH_4^+ and the accumulation of 22.8 – 25.5 mmol L^{-1} NO_2^- in the growth
153 medium. The culture was continuously grown under these conditions for 10 days.

154 Sterile samples (~5 mL) were taken on a daily basis. Culture purity was assessed by periodically
155 inoculating ~100 µl of culture onto lysogeny broth (Sigma-Aldrich) agar plates, which were incubated at
156 30°C for at least 4 days. Any observed growth on agar plates was considered to be a contamination and
157 those cultures were discarded. NH_4^+ and NO_2^- concentrations were determined colorimetrically (55) and
158 cell density was determined spectrophotometrically (Beckman) by making optical density measurements
159 at 600 nm (OD_{600}) (Table S1). Total biomass in grams dry cell weight per liter (gDCW L^{-1}), substrate-
160 consumption rate (q_{NH_3}), and apparent growth yield (Y) were calculated as described in Mellbye *et al.*
161 (2016). To test for statistically significant differences in NH_4^+ to NO_2^- conversion stoichiometry, q_{NH_3}, and
162 Y between NH_3- and O_2-limited steady-state growth, a Welch's t-test was performed.
163

164 **2.2 RNA extraction and transcriptome sequencing**

165 For RNA extraction and transcriptome sequencing, three replicate samples (40 mL) were
166 collected on three separate days during NH_3-limited (days 9, 10, 11) and O_2-limited (days 28, 29, 30)
167 steady-state growth (Fig. 2). The samples were harvested by centrifugation (12,400 x g, 30 min, 4ºC),
168 resuspended in RNeasy RLT buffer with 2-mercaptoethanol, and lysed with an ultrasonication probe (3.5
169 output, Pulse of 30 sec on / 30 sec off for 1 min; Heatsystems Ultrasonic Processor XL). RNA was
170 extracted using the RNeasy minikit (Qiagen) followed by the MICROBExpress-bacteria RNA Purification
171 Kit (Ambion/Life technologies) following the manufacturer's instructions. Depleted RNA quality was
172 assessed using the Bioanalyzer 6000 Nano Lab-Chip Kit (Agilent Technologies). Sequencing libraries
173 were constructed from at least 200 ng rRNA-depleted RNA with the TruSeq targeted RNA expression Kit

(Illumina), and 100 bp paired-end libraries were sequenced on a HiSeq 2000 (Illumina) at the Center for Genome Research and Biocomputing Core Laboratories (CGRB) at Oregon State University.

2.3 Transcriptome analysis

Paired-end transcriptome sequence reads were processed and mapped to open reading frames (ORFs) deposited at NCBI for the *N. europaea* ATCC 19718 (NC_004757.1) reference genome using the CLC Genomics Workbench (CLC bio) under default parameters as previously described (43). Residual reads mapping to the rRNA operon were excluded prior to further analysis. An additive consensus read count was manually generated for all paralogous genes. Thereafter, mapped read counts for each gene were normalized to the gene length in kilobases, and the resulting read per kilobase (RPK) values were converted to transcripts per million (TPM) (56). To test for statistically significant differences between transcriptomes obtained from NH_3- and O_2-limited steady-state growth, TPMs of biological triplicate samples were used to calculate p-values based on a Welch's t-test. The more stringent Welch's, rather than the Student's t-Test was selected due to the limited number of biological replicates (57). Additionally, linear fold changes between average TPMs under both growth conditions for each expressed ORF were calculated. Transcripts with a p-value ≤0.05 and a transcription fold change of ≥1.5x between conditions were considered to be present at significantly different levels.

All retrieved transcriptome sequence data has been deposited in the European Nucleotide Archive (ENA) under the project accession number PRJEB31097.

3 Results and discussion

3.1 Growth characteristics

N. europaea was grown as a continuous steady-state culture under both NH_3- and O_2-limited growth conditions. During NH_3-limited steady-state growth, the culture was kept oxic with a constant supply of filtered atmospheric air, was continuously stirred (400 rpm), and contained a standing NO_2^- concentration of ~60mmol L^{-1}. In contrast, during O_2-limited steady-state growth, no additional air inflow

200 was provided, but the stirring was increased (800 rpm) to facilitate O_2 transfer between the headspace
201 and growth medium. As a consequence of O_2 limitation, the medium contained standing concentrations
202 (~30mmol L^{-1}) of both NH_4^+ and NO_2^- (Fig. 2, Table 1).

203 During NH_3-limited steady-state growth (days 7-16; Fig. 2), *N. europaea* stoichiometrically
204 oxidized all supplied NH_4^+ to NO_2^- (N-balance = 61.0 ±1.7 mmol L^{-1}) and maintained an OD_{600} of 0.15
205 ±0.01 (Table 1). During O_2-limited steady-state growth (days 23-32; Fig. 2), *N. europaea* was able to
206 consume on average 31.1 ±1.5 mmol L^{-1} (51.8%) of the supplied NH_4^+, and maintained an OD_{600} of 0.07
207 ±0.01 (Table 1). A decrease in OD_{600} was expected, as the O_2-limited culture oxidized less total
208 substrate (NH_4^+), resulting in less biomass produced. The conversion of NH_4^+ to NO_2^- was not
209 stoichiometric during O_2-limited growth, as only 77.5% (24.1 ±0.8 mmol L^{-1}) of the NH_4^+ oxidized was
210 measured as NO_2^- in the effluent, resulting in an N-balance of 52.8 ±1.8 mmol L^{-1} (Table 1). The
211 significant difference ($p \leq 0.01$) in the N-balance between NH_4^+ consumed and NO_2^- formed during O_2-
212 limited growth is in accordance with previous reports and likely due to increased N-loss in the form of
213 NH_2OH, NO, and N_2O during O_2-limited conditions (12, 35, 42, 58).

214 The dilution rate (0.01 h^{-1}) of the chemostat was kept constant during both NH_3- and O_2-limited
215 growth, and resulted in 14.4 mmol day^{-1} NH_4^+ delivered into the chemostat. On days (9, 10, and 11),
216 which were sampled for NH_3-limited growth transcriptomes, *N. europaea* consumed NH_3 at a rate (q_{NH_3})
217 of 24.73 ±0.53 mmol $gDCW^{-1}$ h^{-1} with an apparent growth yield (Y) of 0.40 ±0.01 gDCW mol^{-1} NH_3.
218 During days (28, 29, and 30) sampled for O_2-limited growth transcriptomes, the q_{NH_3} was significantly
219 higher (28.51 ±1.13 mmol $gDCW^{-1}$ h^{-1}; $p \leq 0.05$), while Y was significantly lower (0.35 ±0.01 gDCW mol^{-1}
220 NH_3; $p \leq 0.05$). When the whole ten day NH_3- and O_2-limited steady-state growth periods are considered
221 the q_{NH_3} and Y trends remain statistically significant ($p \leq 0.05$) (Table 1). Overall, NH_3 oxidation was less
222 efficiently coupled to biomass production under O_2-limited growth conditions.
223

3.2 Global transcriptomic response of *N. europaea* to growth under NH_3- versus O_2-limited conditions

Under both NH_3- and O_2-limited growth conditions, transcripts mapping to 2535 out of 2572 protein coding genes (98.5%) and 3 RNA coding genes (*ffs*, *rnpB*, and tmRNA) were detected. Many of the 37 genes not detected here encode phage elements or transposases, some of which may have been excised from the genome in the >15 years of culturing since genome sequencing (File S1). In addition, no tRNA transcripts were detected. The high proportion of transcribed genes is in line with recent *N. europaea* transcriptomic studies, where similarly high fractions of transcribed genes were detected (43, 48). A significant difference in transcript levels between growth conditions was detected for 615 (~24%) of transcribed genes (Fig. S1). Of these 615 genes, 435 (~71%) were present at higher levels, while 180 (~29%) were present at lower levels during O_2-limited growth. Genes encoding hypothetical proteins with no further functional annotation accounted for ~21% (130) of the differentially transcribed genes (File S1). Steady-state growth under O_2-limited conditions mainly impacted the transcription of genes in clusters of orthologous groups (COGs) related to transcription and translation, ribosome structure and biogenesis, carbohydrate transport and metabolism, as well as energy production and conversion (Fig. 3).

3.3 Universal and reactive oxygen stress

The transcript levels of various chaperone proteins and sigma factors considered to be involved in general stress response in *N. europaea* (45) differed between NH_3- and O_2-limited growth with no discernible trend of regulation (Table S2, File S1). Overall, prolonged exposure to O_2 limitation did not seem to induce a significantly increased general stress response in *N. europaea*. Key genes involved in oxidative stress defense (superoxide dismutase, catalase, peroxidases, and thioredoxins) were transcribed at lower levels during O_2-limited growth, as expected (Table S2, File S1). Surprisingly, rubredoxin (NE1426) and a glutaredoxin family protein-encoding gene (NE2328) did not follow this trend and were transcribed at significantly higher levels (2.8- and 1.8-fold, respectively) during O_2-limited

growth (Table S2). Although their role in *N.* europaea is currently unresolved, both have been proposed to be involved in cellular oxidative stress response (60, 61), iron homeostasis (62, 63) or both.

3.4 Carbon fixation, carbohydrate and storage compound metabolism

There was a particularly strong effect of O_2-limited growth on the transcription of several genes related to CO_2 fixation (Fig. 3b). The four genes of the RuBisCO-encoding *cbb* operon (*cbbOQSL*) were among the genes displaying the largest decrease in detected transcript numbers (Fig. 4; Table S2). Correspondingly, the transcriptional repressor of the *cbb* operon (*cbbR*) was transcribed at 4.5-fold higher levels (Fig. 4, Table S2). This agrees with the previously reported decrease in transcription of the *N. europaea cbbOQSL* operon in O_2-limited batch culture experiments (64). The reduced transcription of RuBisCO-encoding genes potentially reflects a decreased RuBisCO enzyme concentration needed to maintain an equivalent CO_2 fixation rate during O_2-limited growth. Since O_2 acts as a competing substrate for the RuBisCO active site, the CO_2 fixing carboxylase reaction proceeds more efficiently at lower O_2 concentrations (53, 65, 66). When *N. europaea* is grown under CO_2 limitation, the transcription of RuBisCO encoding genes increases significantly (43, 64, 67). Due to the absence of carboxysomes, *N. europaea* appears to regulate CO_2 fixation at the level of RuBisCO enzyme concentration.

Genes encoding the remaining enzymes of the CBB pathway and carbonic anhydrases were not significantly differentially regulated with the exception of the transketolase-encoding *cbbT* gene (Table S2). Likewise, almost no differences in transcription were observed for the majority of genes in other central metabolic pathways (glycolysis/gluconeogenesis, TCA cycle; File S1). As the specific growth rate of *N. europaea* was kept constant during both NH_3- and O_2-limited growth, it is not surprising that genes associated with these core catabolic pathways were transcribed at comparable levels.

Differential transcription of polyphosphate (PP) metabolism-related genes suggests an increased accumulation of PP storage during O_2-limited growth. Transcripts of the polyphosphate kinase (*ppk*) involved in PP synthesis were detected in significantly higher numbers (2.1-fold), while transcription of the gene encoding the PP-degrading exopolyphosphatase (*ppx*) did not change (Table S2). Indeed, *N.*

europaea has previously been shown to accumulate PP when ATP generation (NH_3 oxidation) and ATP consumption become uncoupled and surplus ATP is available (68). As the specific growth rate was kept constant throughout the experiment, PP accumulation could be a result of increased efficiency in ATP-consuming pathways, like CO_2 fixation or oxidative stress induced repair. A decrease in the reaction flux through the energetically wasteful oxygenase reaction catalyzed by RuBisCO could result in surplus ATP being diverted to PP production.

3.5 Energy conservation

Genes encoding the known core enzymes of the NH_3 oxidation pathway in *N. europaea* were all highly transcribed during both NH_3- and O_2-limited growth (Table S2). These included the ammonia monooxygenase (AMO; *amoCAB* operons and the singleton *amoC* gene), as well as the HAO (*haoBA*) and the accessory cyt c_{554} (*cycA*) and cyt c_{m552} (*cycX*) encoding genes. Due to a high level of sequence conservation among the multiple AMO and HAO operons (69), it is not possible to decipher the transcriptional responses of paralogous genes in these clusters. Therefore, we report the regulation of AMO and HAO operons as single units (Table S2). The transcript numbers of genes in the AMO operons decreased up to 3.3-fold during O_2-limited growth, while transcripts of the singleton *amoC* were present at 1.9-fold higher levels. However, these transcriptional differences were not statistically significant. The HAO cluster genes were also not significantly differentially transcribed (Table S2).

Previous research has shown that transcription of AMO, and to a lesser extent of HAO, is induced by NH_3 in a concentration dependent manner (70). In contrast, other studies have reported an increase in *amoA* transcription by *N. europaea* following substrate limitation (44, 71). Furthermore, *N. europaea* has been reported to increase *amoA* and *haoA* transcription during growth under low O_2 conditions (34). However, exposure to repeated transient anoxia did not significantly change *amoA* or *haoA* mRNA levels (36). As both NH_3- and O_2 limitation have previously been shown to induce transcription of AMO and HAO encoding genes, the high transcription levels observed here under both NH_3- and O_2-limited steady-state growth conditions are not surprising.

The periplasmic red copper protein nitrosocyanin (NcyA) was among the most highly transcribed genes under both NH_3- and O_2-limited growth conditions (Table S2). Nitrosocyanin has been shown to be expressed at levels similar to other nitrification and electron transport proteins (72), and is among the most abundant proteins commonly found in AOB proteomes (47, 73). To date, the nitrosocyanin encoding gene *ncyA* has been identified only in AOB genomes (24), and has been proposed as a candidate for the nitric oxide oxidase (40). However, as comammox *Nitrospira* do not encode *ncyA* (2, 3, 13), and neither do all genome sequenced AOB (74), nitrosocyanin cannot be the NO oxidase in all ammonia oxidizers. In this study, a slight (1.7-fold), but not statistically significantly higher number of *ncyA* transcripts was detected during O_2-limited growth (Table S2). This agrees with a previous study comparing *ncyA* mRNA levels in *N. europaea* continuous cultures grown under high and low O_2 conditions (44). However, *N. europaea* performing pyruvate-dependent NO_2^- reduction also significantly upregulated *ncyA*, while transcription of *amoA* and *haoA* decreased (44). Overall, there is evidence for an important role of nitrosocyanin in NH_3 oxidation or electron transport in AOB, but further experiments are needed to elucidate its exact function.

Three additional cytochromes are considered to be involved in the ammonia-oxidizing pathway of *N. europaea*: i) cyt c_{552} (*cycB*), essential for electron transfer; ii) cyt P460 (*cytL*), responsible for N_2O production from NO and hydroxylamine (39); and iii) cyt *c*'-beta (*cytS*), hypothesized to be involved in N-oxide detoxification and metabolism (24, 75). All three were among the most highly transcribed genes (top 20%) under both growth conditions (Table S2). In this study, *cytS* was transcribed at significantly lower levels (2.3-fold) during O_2-limited growth. However, transcription of *cycB* and *cytL* were not significantly different (Table S2). While the *in vivo* function of *cytS* remains elusive, it is important to note that in contrast to *ncyA*, the *cytS* gene is present in all sequenced AOB and comammox *Nitrospira* genomes (12, 13, 52). The ubiquitous detection of *cytS* in genomes of all AOB, comammox *Nitrospira*, and in methane-oxidizing bacteria capable of NH_3 oxidation (76), indicates that cyt *c*'-beta might play an important, yet unresolved role in bacterial aerobic NH_3 oxidation.

3.6 Nitrifier denitrification

During O_2-limited growth, *N. europaea* either performs nitrifier denitrification or experiences a greater loss of N intermediates like NH_2OH (59) or NO (20), which leads to the observed N-imbalance between total NH_4^+ consumed and NO_2^- produced (Fig. 2, Table 1). The Cu-containing NO_2^- reductase NirK and the iron-containing membrane-bound cyt *c* dependent NO reductase (cNOR; NorBC) are considered to be the main nitrifier denitrification enzymes (24, 35). *N. europaea* NirK plays an important role in both nitrifier denitrification and NH_3 oxidation (27), and is known to be expressed during both O_2-replete and -limited growth (29, 30, 35). However, under O_2-limited conditions, *nirK* was amongst the genes with the largest decrease in transcript numbers (4.2-fold) observed in this study (Fig. 5, Table S2). In *N. europaea*, *nirK* transcription is regulated via the nitrite-sensitive transcriptional repressor *nsrA* (30). Thus, in contrast to the *nirK* of many denitrifiers (77), *nirK* transcription in *N. europaea* is regulated in response to NO_2^- concentration and not NO or O_2 availability (31, 34, 48). The reduced O_2 supply during O_2-limited growth resulted in a ~50% decrease in total NH_3 oxidized and a ~60% reduction in steady-state NO_2^- concentration (Fig. 2, Table 1). The decrease in NO_2^- concentration during O_2-limited growth likely induced the transcription of *nsrA*, which was significantly (2.1-fold) upregulated (Fig. 5, Table S2). Therefore the large decrease in *nirK* transcription observed here may be due to the lower NO_2^- concentrations and not a direct reflection of overall nitrifier denitrification activity. This hypothesis is consistent with the observation that NirK is not essential for NO_2^- reduction to NO in *N. europaea*, and the presence of a not yet identified nitrite reductase in this organism. Previously, it has been shown that *N. europaea nirK* knockout mutants are still able to enzymatically produce NO and N_2O (29, 35), even if hydrazine is oxidized by HAO instead of hydroxylamine as an electron donor (35). In addition, NO and N_2O formation has also been observed in the AOB *Nitrosomonas communis* that does not encode *nirK* (12). The other three genes in the NirK cluster (*ncgCBA*) were differentially transcribed, with *ncgC* and *ncgB* being transcribed at lower levels (2 and 1.3-fold respectively), while *ncgA* was transcribed at a significantly higher level (2.6-fold) during O_2-limited growth. The role of *ncgCBA* in *N. europaea* has not

353 been fully elucidated, but all three genes have previously been implicated in the metabolism or tolerance
354 of N-oxides and NO_2^- (31).

355 In contrast, transcripts of the *norCBQD* gene cluster, encoding for the iron-containing, cyt *c*
356 dependent cNOR type NO reductase, were present at slightly higher (1.2- to 1.5-fold) but not significantly
357 different levels during O_2-limited growth (Fig. 5, Table S2). Previous research has demonstrated that in
358 *N. europaea* cNOR functions as the main NO reductase under anoxic and hypoxic conditions (35).
359 Interestingly, all components of the proposed alternative heme-copper containing NO reductase (sNOR),
360 including the NO/low oxygen sensor *senC* (24) were transcribed at significantly higher levels (2.7- to
361 10.8-fold) during O_2-limited growth (Fig. 6, Table S2). Therefore, it is possible that the phenotype
362 describing cNOR as the main NO reductase in *N. europaea* (35) was a product of short incubation times
363 and that during longer term O_2-limited conditions sNOR contributes to NO reduction during nitrifier
364 denitrification. Another possibility is that the increased transcription of sNOR observed here during O_2-
365 limited growth is primarily related to respiration and not NO reductase activity.
366

367 **3.7 Respiratory chain and terminal oxidases**

368 *N. europaea* encodes a low affinity cyt *c* aa3 (A1-type) HCO, but not a high affinity *cbb*$_3$-type (C-
369 type) cyt *c* HCO encoded by other AOB such as *N. eutropha* or *Nitrosomonas* sp. GH22 (28, 50, 52).
370 Significantly higher numbers of transcripts (1.7- to 3.0-fold) of all three subunits of the cyt *c* *aa*$_3$ HCO and
371 the cyt *c*-oxidase assembly gene *ctaG* were detected during O_2-limited growth (Fig. 6, Table S2).
372 Increased transcription of the terminal oxidase was expected, as it is a common bacterial response to O_2
373 limitation (78). In addition, transcripts of all three subunits of the proton translocating cyt *bc*1 complex
374 (Complex III) were present in higher numbers (Table S2). The NADPH dehydrogenase (Complex I) and
375 the ATP synthase (Complex V) encoding genes were transcribed at similar levels during both growth
376 conditions (Table S2).

377 As mentioned above, transcripts of both subunits of sNOR (*norSY* previously called *coxB*$_2$*A*$_2$),
378 and the NO/low oxygen sensor *senC* were present at significantly higher numbers (2.7- to 10.8-fold)

during O_2-limited growth (Fig. 6, Table S2). The NO reductase function of the sNOR enzyme complex was proposed based on domain similarities between NorY and NorB (24, 32). Yet, *norY* phylogenetically affiliates with and structurally resembles B-type HCOs (79). In addition, NorY does not contain the five well-conserved and functionally important NorB glutamate residues (80), which are present in the canonical NorB of *N. europaea*. All HCOs studied thus far can reduce O_2 to H_2O, and couple this reaction to proton translocation, albeit B- and C-type HCOs translocate fewer protons per mol O_2 reduced than A-type HCOs (81). Notably, NO reduction to N_2O is a known side reaction of the A2-, B- and C-, but not A1-type HCOs (82-84). The transcriptional induction of sNOR during O_2-limited growth reported here, as well as the high O_2 affinity of previously studied B-type HCOs (85) indicate that sNOR might function as a high affinity terminal oxidase in *N. europaea* and possibly other sNOR-encoding AOB. Furthermore, functionally characterized B-type HCOs display a lower NO turnover rate than the more widespread high affinity C-type HCOs (82, 83). Taken together, these observations indicate that B-type HCOs, like sNOR, are ideal for scavenging O_2 during O_2-limited growth conditions that coincide with elevated NO concentrations, which would impart a fitness advantage for AOB growing under these conditions. Lastly, the NOR of *Roseobacter denitrificans* structurally resembles cNOR, but contains a HCO-like heme-cooper center in place of the heme-iron center of canonical cNORs. Interestingly, this cNOR readily reduces O_2 to H_2O, but displays very low NO reductase activity (86, 87). Therefore, in line with previous hypotheses (82, 86), the presence of a heme-copper center in NOR/HCO superfamily enzymes, such as the sNOR of *N. europaea,* may indicate O_2 reduction as the primary enzymatic function. Notably, a recent study provided the first indirect evidence of NO reductase activity of sNOR in the marine NOB, *Nitrococcus mobilis* (88). However, further research is needed to resolve the primary function of sNOR in nitrifiying microorganisms.

4 Conclusions

In this study, we examined the transcriptional response of *N. europaea* to continuous growth under steady-state NH_3- and O_2-limited conditions. Overall, O_2-limited growth resulted in a decreased

405 growth yield, but did not invoke a significant stress response in *N. europaea*. On the contrary, a reduced
406 need for oxidative stress defense was evident. Interestingly, no clear differential regulation was observed
407 for genes classically considered to be involved in aerobic NH_3 oxidation. In contrast, a strong decrease
408 in transcription of RuBisCO encoding genes during O_2-limited growth was observed, suggesting that
409 control of CO_2 fixation in *N. europaea* is exerted at the level of RuBisCO enzyme concentration.
410 Futhermore, the remarkably strong increase in transcription of the genes encoding for sNOR (B-type
411 HCO) indicates this enzyme complex might function as a high-affinity terminal oxidase in *N. europaea*
412 and other AOB. Overall, despite lower growth yield, *N. europaea* successfully adapts to growth under
413 hypoxic conditions by regulating core components of its carbon fixation and respiration machinery.
414

415 **Acknowledgements**

416 We thank the Center for Genome Research and Biocomputing at Oregon State University for the
417 sequencing services. We also thank Fillipa Sousa for helpful discussions. This work was funded by
418 Department of Energy (DOE) award ER65192 (co-principal investigators, L.A.S-S. and P.J.B.). C.J.S.,
419 H.D., and M.W. were supported by the Comammox Research Platform of the University of Vienna. In
420 addition, M.W. and C.J.S. were supported by the European Research Council (ERC) via the Advanced
421 Grant project NITRICARE 294343, and C.J.S. and H.D. were supported by Austrian Science Fund
422 (FWF) grant 30570-B29. A.T.G and D.W. were supported by the ERC Starting Grant 636928, under the
423 European Union's Horizon 2020 research and innovation program.
424

References

1. **Kuypers MMM, Marchant HK, Kartal B**. 2018. The microbial nitrogen-cycling network. Nat Rev Microbiol **16**:263–276.
2. **Daims H, Lebedeva EV, Pjevac P, Han P, Herbold C, Albertsen M, Jehmlich N, Palatinszky M, Vierheilig J, Bulaev A, Kirkegaard RH, von Bergen M, Rattei T, Bendinger B, Nielsen PH, Wagner M**. 2015. Complete nitrification by *Nitrospira* bacteria. Nature **528**:504–506.
3. **van Kessel MAHJ, Speth DR, Albertsen M, Nielsen PH, den Camp HJO, Kartal B, Jetten MSM, Lücker S**. 2015. Complete nitrification by a single microorganism. Nature **528**:555–559.
4. **Kitzinger K, Koch H, Lücker S, Sedlacek CJ, Herbold C, Schwarz J, Daebeler A, Mueller AJ, Lukumbuzya M, Romano S, Leisch N, Karst SM, Kirkegaard R, Albertsen M, Nielsen PH, Wagner M, Daims H**. 2018. Characterization of the first "Candidatus Nitrotoga" isolate reveals metabolic versatility and separate evolution of widespread nitrite-oxidizing bacteria. MBio **9**:e01186-18. doi:10.1128/mBio.01186-18.
5. **Galloway JN, Townsend AR, Erisman JW, Bekunda M, Cai Z, Freney JR, Martinelli LA, Seitzinger SP, Sutton MA**. 2008. Transformation of the nitrogen cycle: recent trends, questions, and potential solutions. Science **320**:889–892.
6. **Dundee L, Hopkins DW**. 2001. Different sensitivities to oxygen of nitrous oxide production by *Nitrosomonas europaea* and *Nitrosolobus multiformis*. Soil Biol Biochem **33**:1563–1565.
7. **Shaw LJ, Nicol GW, Smith Z, Fear J, Prosser JI, Baggs EM**. 2006. *Nitrosospira* spp. Can produce nitrous oxide via a nitrifier denitrification pathway. Environ Microbiol **8**:214–222.
8. **Ahn JH, Kwan T, Chandran K**. 2011. Comparison of partial and full nitrification processes applied for treating high-strength nitrogen wastewaters: microbial ecology through nitrous oxide production. Environ Technol **45**:2734–2740.
9. **Kool DM, Dolfing J, Wrage N, Van Groenigen JW**. 2011. Nitrifier denitrification as a distinct and significant source of nitrous oxide from soil. Soil Biol Biochem **43**:174–178.
10. **Santoro AE, Buchwald C, McIlvin MR, Casciotti KL**. 2011. Isotopic signature of N_2O produced by marine ammonia-oxidizing archaea. Science **333**:1282–1285.

11. **Stein LY**. 2011. Surveying N_2O-producing pathways in bacteria, p 131-152. *In* Klotz MG (ed), Methods in enzymology. Academic Press, CA.
12. **Kozlowski JA, Kits KD, Stein LY**. 2016. Comparison of nitrogen oxide metabolism among diverse ammonia-oxidizing bacteria. Front Microbiol **7**:1090. doi:10.3389/fmicb.2016.01090.
13. **Kits KD, Jung MY, Vierheilig J, Pjevac P, Sedlacek CJ, Liu S, Herbold C, Stein LY, Richter A, Wissel H, Brüggemann N, Wagner M, Daims H**. 2019. Low yield and abiotic origin of N_2O formed by the complete nitrifier *Nitrospira inopinata.* Nat Commun **10**:1836. doi:10.1038/s41467-019-09790-x.
14. **Schreiber F, Wunderlin P, Udert KM, Wells GF**. 2012. Nitric oxide and nitrous oxide turnover in natural and engineered microbial communities: biological pathways, chemical reactions, and novel technologies. Front Microbiol **3**:372. doi: 10.3389/fmicb.2012.00372.
15. **Heil J, Vereecken H, Brüggemann N**. 2016. A review of chemical reactions of nitrification intermediates and their role in nitrogen cycling and nitrogen trace gas formation in soil. Eur J Soil Sci **67**:23–39.
16. **Hooper AB**. 1968. A nitrite-reducing enzyme from *Nitrosomonas europaea*. Preliminary characterization with hydroxylamine as electron donor. Biochim Biophys Acta **162**:49–65.
17. **Hooper AB, Terry KR**. 1977. Hydroxylamine oxidoreductase from *Nitrosomonas*: inactivation by hydrogen peroxide. Biochem Moscow **16**:455–459.
18. **Hooper AB, Terry KR, Maxwell PC**. 1977. Hydroxylamine oxidoreductase of *Nitrosomonas*. Oxidation of diethyldithiocarbamate concomitant with stimulation of nitrite synthesis. Biochim Biophys Acta **462**:141–152.
19. **Anderson IC, Poth M, Homstead J, Burdige D**. 1993. A comparison of NO and N_2O production by the autotrophic nitrifier *Nitrosomonas europaea* and the heterotrophic nitrifier *Alcaligenes faecalis*. Appl Environ Microbiol **59**:3525–3533.
20. **Caranto JD, Lancaster KM**. 2017. Nitric oxide is an obligate bacterial nitrification intermediate produced by hydroxylamine oxidoreductase. PNAS **114**:8217–8222.

21. **Mellbye BL, Giguere AT, Murthy GS, Bottomley PJ, Sayavedra-Soto LA, Chaplen FW**. 2018. Genome-scale, constraint-based modeling of nitrogen oxide fluxes during coculture of *Nitrosomonas europaea* and *Nitrobacter winogradskyi*. mSystems **3**:e00170-17. doi:10.1128/mSystems.00170-17.

22. **Poth M, Focht DD**. 1985. 15N kinetic analysis of N_2O production by *Nitrosomonas europaea*: an examination of nitrifier denitrification. Appl Environ Microbiol **49**:1134–1141.

23. **Wrage N, Velthof GL, van Beusichem ML, Oenema O**. 2001. Role of nitrifier denitrification in the production of nitrous oxide. Soil Biol Biochem **33**:1723–1732.

24. **Klotz MG, Stein LY**. 2008. Nitrifier genomics and evolution of the nitrogen cycle. FEMS Microbiol Lett **278**:146–156.

25. **Giguere AT, Taylor AE, Suwa Y, Myrold DD, Bottomley PJ**. 2017. Uncoupling of ammonia oxidation from nitrite oxidation: impact upon nitrous oxide production in non-cropped Oregon soils. Soil Biol Biochem **104**:30–38.

26. **Schmidt I, van Spanning RJM, Jetten MSM**. 2004. Denitrification and ammonia oxidation by *Nitrosomonas europaea* wild-type, and NirK- and NorB-deficient mutants. Microbiology **150**:4107–4114.

27. **Cantera JJL, Stein LY**. 2007. Role of nitrite reductase in the ammonia-oxidizing pathway of *Nitrosomonas europaea*. Arch Microbiol **188**:349–354.

28. **Chain P, Lamerdin J, Larimer F, Regala W, Lao V, Land M, Hauser L, Hooper A, Klotz M, Norton J, Sayavedra-Soto L, Arciero D, Hommes N, Whittaker M, Arp D**. 2003. Complete genome sequence of the ammonia-oxidizing bacterium and obligate chemolithoautotroph *Nitrosomonas europaea*. J Bacterial **185**:2759–2773.

29. **Beaumont HJ, Hommes NG, Sayavedra-Soto LA, Arp DJ, Arciero DM, Hooper AB, Westerhoff HV, van Spanning RJM**. 2002. Nitrite reductase of *Nitrosomonas europaea* is not essential for production of gaseous nitrogen oxides and confers tolerance to nitrite. J Bacteriol **184**:2557–2560.

30. **Beaumont HJ, Lens SI, Reijnders WN, Westerhoff HV, van Spanning RJ**. 2004. Expression of nitrite reductase in *Nitrosomonas europaea* involves NsrR, a novel nitrite-sensitive transcription repressor. Mol Microbiol **54**:148–158.

31. **Beaumont HJ, Lens SI, Westerhoff HV, van Spanning RJ**. 2005. Novel *nirK* cluster genes in *Nitrosomonas europaea* are required for NirK-dependent tolerance to nitrite. J Bacteriol **187**:6849–6851.

32. **Cho CMH, Yan T, Liu X, Wu L, Zhou J, Stein LY**. 2006. Transcriptome of a *Nitrosomonas europaea* mutant with a disrupted nitrite reductase gene (*nirK*). Appl Environ Microbiol **72**:4450–4454.

33. **Pellitteri-Hahn MC, Halligan BD, Scalf M, Smith L, Hickey WJ**. 2011. Quantitative proteomic analysis of the chemolithoautotrophic bacterium *Nitrosomonas europaea*: comparison of growing- and energy-starved cells. J Proteomics **74**:411–419.

34. **Yu R, Chandran K**. 2010. Strategies of *Nitrosomonas europaea* 19718 to counter low dissolved oxygen and high nitrite concentrations. BMC Microbiol, **10**:70. doi: 10.1186/1471-2180-10-70.

35. **Kozlowski JA, Price J, Stein LY**. 2014. Revision of N_2O-producing pathways in the ammonia-oxidizing bacterium, *Nitrosomonas europaea* ATCC 19718. Appl Environ Microbiol **80**:4930-4935.

36. **Yu R, Perez-Garcia O, Lu H, Chandran, K**. 2018. *Nitrosomonas europaea* adaptation to anoxic-oxic cycling: insights from transcription analysis, proteomics and metabolic network modeling. Sci Total Environ **615**:1566–1573.

37. **Cua LS, Stein LY**. 2011. Effects of nitrite on ammonia-oxidizing activity and gene regulation in three ammonia-oxidizing bacteria. FEMS Microbial Lett **319**:169-175.

38. **Upadhyay AK, Hooper AB, Hendrich MP**. 2006. NO reductase activity of the tetraheme cytochrome C_{554} of *Nitrosomonas europaea*. J Am Chem Soc **128**:4330-4337.

39. **Caranto JD, Vilbert AC, Lancaster KM**. 2016. *Nitrosomonas europaea* cytochrome P460 is a direct link between nitrification and nitrous oxide emission. PNAS **113**:14704–14709.

40. **Lancaster KM, Caranto JD, Majer SH, Smith MA**. 2018. Alternative Bioenergy: Updates to and challenges in nitrification metalloenzymology. Joule **2**:421–441.

41. **McGarry JM, Pacheco A**. 2018. Upon further analysis, neither cytochrome c554 from *Nitrosomonas europaea* nor its F156A variant display NO reductase activity, though both proteins bind nitric oxide reversibly. J Biol Inorg Chem **23**:861–878.

42. **Kester RA, De Boer W, Laanbroek HJ**. 1997. Production of NO and N_2O by pure cultures of nitrifying and denitrifying bacteria during changes in aeration. Appl Environ Microbiol **63**:3872–3877.

43. **Mellbye BL, Giguere A, Chaplen F, Bottomley PJ, Sayavedra-Soto LA**. 2016. Steady state growth under inorganic carbon limitation increases energy consumption for maintenance and enhances nitrous oxide production in *Nitrosomonas europaea*. Appl Environ Microbiol **82**:3310 – 3318.

44. **Beyer S, Gilch S, Meyer O, Schmidt I**. 2009. Transcription of genes coding for metabolic key functions in *Nitrosomonas europaea* during aerobic and anaerobic growth. J Mol Microbiol Biotechnol **16**:187–197.

45. **Gvakharia BO, Permina EA, Gelfand MS, Bottomley PJ, Sayavedra-Soto LA, Arp DJ**. 2007. Global transcriptional response of *Nitrosomonas europaea* to chloroform and chloromethane. Appl Environ Microbiol **73**:3440–3445.

46. **Park S, Ely RL**. 2008. Genome-wide transcriptional responses of *Nitrosomonas europaea* to zinc. Arch Microbiol **189**:541–548.

47. **Kartal B, Wessels HJ, van der Biezen E, Francoijs KJ, Jetten MS, Klotz MG, Stein LY**. 2012. Effects of nitrogen dioxide and anoxia on global gene and protein expression in long-term continuous cultures of *Nitrosomonas eutropha* C91. Appl Environ Microbiol **78**:4788-4794.

48. **Pérez J, Buchanan A, Mellbye B, Ferrell R, Chang JH, Chaplen F, Bottomley PJ, Arp DJ, Sayavedra-Soto LA**. 2015. Interactions of *Nitrosomonas europaea* and *Nitrobacter winogradskyi* grown in co-culture. Arch Microbiol **197**:79–89.

49. **Sayavedra-Soto LA, Arp DJ. 2011.** Ammonia-oxidizing Bacteria: Their biochemistry and molecular biology, p 11-38. *In* Nitrification, Ward BB, Arp DJ, Klotz MG (eds). ASM, Washington, DC.

50. **Stein LY, Arp DJ, Berube PM, Chain PS, Hauser L, Jetten MS, Klotz MG, Larimer FW, Norton JM, op den Camp HJ, Shin M, Wei X**. 2007. Whole-genome analysis of the ammonia-oxidizing bacterium, *Nitrosomonas eutropha* C91: implications for niche adaptation. Environ Microbiol **9**:2993–3007.

51. **Berg IA. 2011.** Ecological aspects of the distribution of different autotrophic CO_2 fixation pathways. Appl Environ Microbiol **77**:1925-1936.

52. **Sedlacek CJ, McGowan B, Suwa Y, Sayavedra-Soto LA, Laanbroek HJ, Stein LY, Norton JM, Klotz MG, Bollmann A**. 2019. A physiological and genomic comparison of *Nitrosomonas* cluster 6a and 7 ammonia-oxidizing bacteria. Microb Ecol. doi:10.1007/s00248-019-01378-8.

53. **Andrews TJ, Lorimer GH**. 1978. Photorespiration—still unavoidable?. FEBS Lett **90**:1–9.

54. **Badger MR, Bek EJ**. 2008. Multiple RuBisCo forms in proteobacteria: their functional significance in relation to CO_2 acquisition by the CBB cycle. J Exp Bot **59**:1525–1541.

55. **Hood-Nowotny R, Umana NHN, Inselbacher E, Oswald-Lachouani P, Wanek W**. 2010. Alternative methods for measuring inorganic, organic, and total dissolved nitrogen in soil. Soil Sci Soc Am J **74**:1018–1027.

56. **Li B, Ruotti V, Stewart RM, Thomson JA, Dewey CN**. 2010. RNA-Seq gene expression estimation with read mapping uncertainty. Bioinformatics **26**:493–500.

57. **Götz F, Pjevac P, Markert S, McNichol J, Becher D, Schweder T, Mussmann M, Sievert SM**. 2018. Transcriptomic and proteomic insight into the mechanism of cyclooctasulfur- versus thiosulfate-oxidation by the chemolithoautotroph *Sulfurimonas denitrificans*. Environ Microbiol **21**:244–258.

58. **Goreau TJ, Kaplan WA, Wofsy SC, McElroy MB, Valois FW, Watson SW**. 1980. Production of NO_2^- and N_2O by nitrifying bacteria at reduced concentrations of oxygen. Appl Environ Microbiol **40**:526–532.

59. **Liu S, Han P, Hink L, Prosser JI, Wagner M, Brüggemann N**. 2017. Abiotic conversion of extracellular NH_2OH contributes to N_2O emission during ammonia oxidation. Environ Sci Technol **51**:13122-13132.

60. **Prieto-Alamo MJ, Jurado J, Gallardo-Madueno R, Monje-Casas F, Holmgren A, Pueyo C**. 2000. Transcriptional regulation of glutaredoxin and thioredoxin pathways and related enzymes in response to oxidative stress. J Biol Chem **275**:13398–13405.

61. **Coulter ED, Kurtz DM Jr**. 2001. A role for rubredoxin in oxidative stress protection in *Desulfovibrio vulgaris*: catalytic electron transfer to rubrerythrin and two-iron superoxide reductase. Arch Biochem Biophys **394**:76-86.

62. **Andrews SC, Robinson AK, Rodriguez-Quinones F**. 2003. Bacterial iron homeostasis. FEMS Microbiol Rev **27**:215-237.

63. **Rouhier N, Couturier J, Johnson MK, Jacquot JP**. 2010. Glutaredoxins: roles in iron homeostasis. Trends Biochem Sci **35**:43. doi:10.1016/j.tibs.2009.08.005.

64. **Wei X, Sayavedra-Soto LA, Arp DJ**. 2004. The transcription of the *cbb* operon in *Nitrosomonas europaea*. Microbiology **150**:1869–1879.

65. **Lorimer GH**. 1981. The carboxylation and oxygenation of ribulose 1,5-bisphosphate: the primary events in photosynthesis and photorespiration. Annu Rev Plant Physiol **32**:349–382.

66. **McNevin D, von Caemmerer S, Farquhar G**. 2006. Determining RuBisCO activation kinetics and other rate and equilibrium constants by simultaneous multiple non-linear regression of a kinetic model. J Exp Bot **57**:3883–3900.

67. **Jiang D, Khunjar WO, Wett B, Murthy SN, Chandran K**. 2015. Characterizing the metabolic trade-off in *Nitrosomonas europaea* in response to changes in inorganic carbon supply. Environ Sci Technol **49**:2523–2531.

68. **Terry KR, Hooper AB**. 1970. Polyphosphate and orthophosphate content of *Nitrosomonas europaea* as a function of growth. J Bacteriol **103**:199–206.

69. **Arp DJ, Sayavedra-Soto LA, Hommes NG**. 2002. Molecular biology and biochemistry of ammonia oxidation by *Nitrosomonas europaea*. Arch Microbiol **178**:250–255.

70. **Sayavedra-Soto LA, Hommes NG, Russell SA, Arp DJ**. 1996. Induction of ammonia monooxygenase and hydroxylamine oxidoreductase mRNAs by ammonium in *Nitrosomonas europaea*. Mol Microbiol **20**:541–548.

71. **Chandran K, Love NG**. 2008. Physiological state, growth mode, and oxidative stress play a role in Cd (II)-mediated inhibition of *Nitrosomonas europaea* 19718. Appl Environ Microbiol **74**:2447–2453.

72. **Whittaker M, Bergmann D, Arciero D, Hooper AB**. 2000. Electron transfer during the oxidation of ammonia by the chemolithotrophic bacterium *Nitrosomonas europaea*. Biochim Biophys Acta Bioenerg **1459**:346–355.

73. **Zorz JK, Kozlowski JA, Stein LY, Strous M, Kleiner M**. 2018. Comparative proteomics of three species of ammonia-oxidizing bacteria. Front Microbiol **9**:938. doi:10.3389/fmicb.2018.00938.

74. **Bollmann A, Sedlacek CJ, Norton J, Laanbroek HJ, Suwa Y, Stein LY, Klotz MG, Arp D, Sayavedra-Soto L, Lu M, Bruce D, Detter C, Tapia R, Han J, Woyke T, Lucas SM, Pitluck S, Pennacchio L, Nolan M, Land ML, Huntemann M, Deshpande S, Han C, Chen A, Kyrpides N, Mavromatis K, Markowitz V, Szeto E, Ivanova N, Mikhailova N, Pagani I, Pati A, Peters L, Ovchinnikova G, Goodwin LA**. 2013. Complete genome sequence of *Nitrosomonas* sp. Is79, an ammonia oxidizing bacterium adapted to low ammonium concentrations. Stand Genomic Sci **7**:469-482.

75. **Elmore BO, Bergmann DJ, Klotz MG, Hooper AB**. 2007. Cytochromes P460 and *c*′-beta; a new family of high-spin cytochromes *c*. FEBS Lett **581**:911–916.

76. **Zahn JA, Arciero DM, Hooper AB, Dispirito AA**. 1996. Cytochrome *c*′ of *Methylococcus capsulatus* Bath. Eur J Biochem **240**:684–691.

77. **Zumft WG**. 1997. Cell biology and molecular basis of denitrification. Microbiol Mol Biol Rev **61**:533–616.

78. **Bueno E, Mesa S, Bedmar EJ, Richardson DJ, Delgado MJ**. 2012. Bacterial adaptation of respiration from oxic to microoxic and anoxic conditions: redox control. Antioxid Redox Sign **16**:819–852.

79. **Sousa FL, Alves RJ, Pereira-Leal JB, Teixeira M, Pereira MM**. 2011. A bioinformatics classifier and database for heme-copper oxygen reductases. PLoS One, 6:e19117. doi:10.1371/journal.pone.0019117.

80. **Hino T, Matsumoto Y, Nagano S, Sugimoto H, Fukumori Y, Murata T, Iwata S, Shiro Y**. 2010. Structural basis of biological N_2O generation by bacterial nitric oxide reducatse. Science **330**:1666-1670.

81. **Sousa FL, Alves RJ, Ribeiro MA, Pereira-Leal JB, Teixeira M, Pereira MM**. 2012. The superfamily of heme–copper oxygen reductases: types and evolutionary considerations. Biochim Biophys Acta Bioenerg **1817**:629–637.

82. **Giuffre A, Stubauer G, Sarti P, Brunori M, Zumft WG, Buse G, Soulimane T**. 1999. The heme-copper oxidases of *Thermus thermophilus* catalyze the reduction of nitric oxide: evolutionary implications. PNAS **96**:14718–14723.

83. **Forte E, Urbani A, Saraste M, Sarti P, Brunori M, Giuffrè A**. 2001. The cytochrome *cbb3* from *Pseudomonas stutzeri* displays nitric oxide reductase activity. Eur J Biochem **268**:6486–6491.

84. **Pereira MM, Teixeira M**. 2004. Proton pathways, ligand binding and dynamics of the catalytic site in haem-copper oxygen reductases: a comparison between the three families. Biochim Biophys Acta Bioenerg **1655**:340–346.

85. **Han H, Hemp J, Pace LA, Ouyang H, Ganesan K, Roh JH, Daldal F, Blanke SR, Gennis RB**. 2011. Adaptation of aerobic respiration to low O_2 environments. PNAS **108**:14109–14114.

86. **Matsuda Y, Inamori KI, Osaki T, Eguchi A, Watanabe A, Kawabata SI, Iba K, Arata H**. 2002. Nitric oxide-reductase homologue that contains a copper atom and has cytochrome *c*-oxidase activity from an aerobic phototrophic bacterium *Roseobacter denitrificans*. J Biochem **131**:791–800.

87. **Zumft WG**. 2005. Nitric oxide reductases of prokaryotes with emphasis on the respiratory, heme–copper oxidase type. J Inorg Biochem **99**:194-215.

88. **Füssel J, Lücker S, Yilmaz P, Nowka B, van Kessel MAHJ, Bourceau P, Hach PF, Littmann S, Berg J, Spieck E, Daims H, Kuypers MMM, Lam P**. 2017. Adaptability as the key to success for the ubiquitous marine nitrite oxidizer *Nitrococcus*. Sci Adv 3:e1700807. doi:10.1126/sciadv.1700807.

665 **Figures and Tables:**

666 **Table 1:** Comparison of *N. europaea* growth characteristics and NH_4^+ to NO_2^- conversion stoichiometry during NH_3- and O_2-limited steady-
667 state growth. Letters *a* and *b* represent highly significant differences ($p \leq 0.01$), and letters *c* and *d* represent significant differences ($p \leq 0.05$)
668 within parameters. Capital letters represent comparisons between 10-day periods, whereas lower case letters represent comparisons
669 between 3-day periods.

	Period [days]	OD_{600}[1]	Input NH_3[2] [mmol day^{-1}]	NH_3 consumed[1] [mmol day^{-1}]	Steady-state[1] NH_4^+ [mmol L^{-1}]	Steady-state[1] NO_2^- [mmol L^{-1}]	N-balance[1,3] [mmol]	Ammonia oxidation rate[1] (q_{NH3}) [mmol $gDCW^{-1}$ h^{-1}]	Apparent growth yield[1] (Y) [gDCW mol^{-1} NH_3]
NH_3-limited growth	7 -16	0.15 +0.01	14.4	14.2 +0.1	0.9 +0.5	60.1 +1.4	61.0 +1.7^A	24.04 +0.93^C	0.42 +0.02^C
	9-11	0.15 ±0.004	14.4	14.2 ±0.1	0.9 ±0.4	59.1 ±1.4	60.0 ±1.8^c	24.73 ±0.53^c	0.40 ±0.01^c
O_2-limited growth	23-32	0.07 +0.01	14.4	7.5 +0.4	28.9 +1.5	24.1 +0.8	52.8 +1.8^B	26.44 +2.28^D	0.38 +0.03^D
	28-30	0.07 ±0.0005	14.4	7.5 ±0.3	28.6 ±1.1	24.3 ±1.4	52.9 ±2.4^d	28.51 ±1.13^d	0.35 ±0.01^d

670 [1]Average values of 3 sampling days or 10 day steady-state period, ± standard deviation (Table S1).
671 [2]The NH_4^+ concentration of the influx medium (60 mmol L^{-1}) multiplied by the influx rate (0.24 L day^{-1}).
672 [3]Sum of effluent NH_4^+ and NO_2^- concentrations.

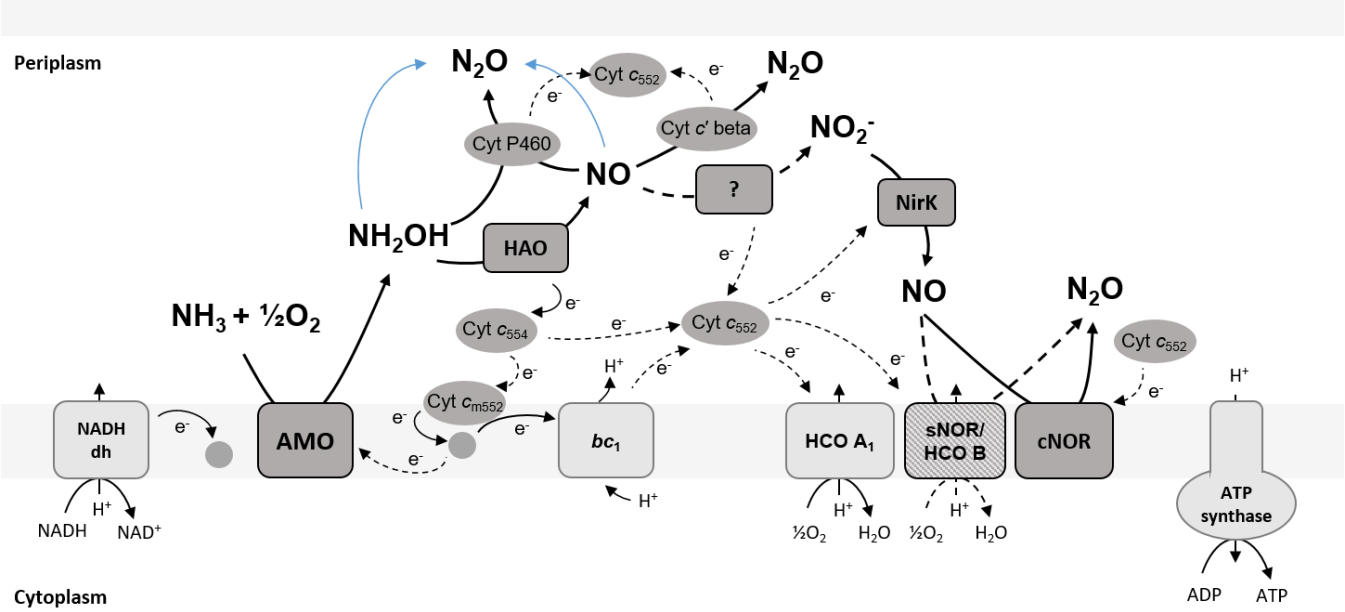

673

674 **Figure 1.** A simplified schematic of electron transport and NO/N_2O producing pathways in *N. europaea*.
675 Solid lines indicate confirmed and dashed lines indicate postulated reactions or electron transfer
676 processes. Abiotic N_2O production is indicated in blue. NADH dh - NADH dehydrogenase (complex I);
677 AMO - ammonia monooxygenase; HAO - hydroxylamine dehydrogenase; NirK - nitrite reductase; *bc*1 -
678 cytrochrome *bc*1 complex (complex III); HCO A1 - heme-copper containing cytochrome *c* oxidase A1-
679 type (complex IV); sNOR/HCO B - heme-copper containing NO reductase/heme-copper containing
680 cytochrome *c* oxidase B-type (complex IV); cNOR - heme-iron containing nitric oxide reductase.

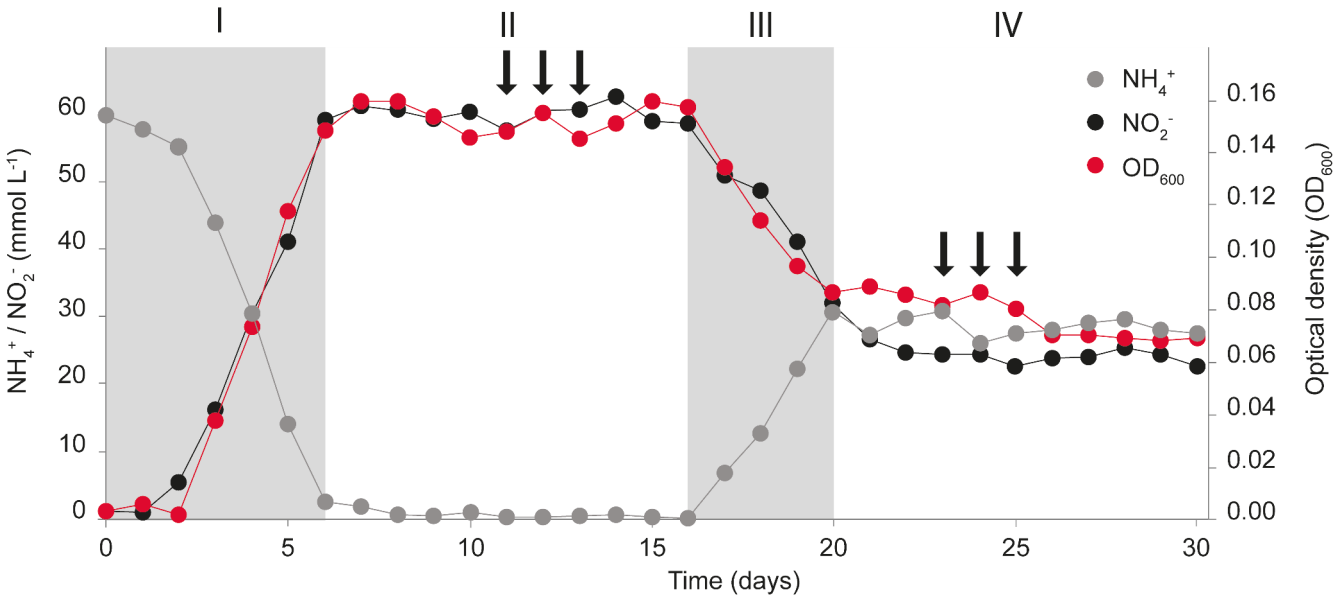

Figure 2. *N. europaea* culture dynamics and sampling scheme. *N. europaea* grown in a chemostat operated: in batch mode (I), under steady-state NH_3-limited conditions as a continuous culture (II), transitioning from NH_3-limited to O_2-limited steady-state growth as a continuous culture (III), and under steady-state O_2-limited conditions as a continuous culture (IV). Arrows indicate transcriptome sampling points during NH_3-limited (days 9, 10 and 11) and O_2-limited (days 28, 29 and 30) steady-state growth.

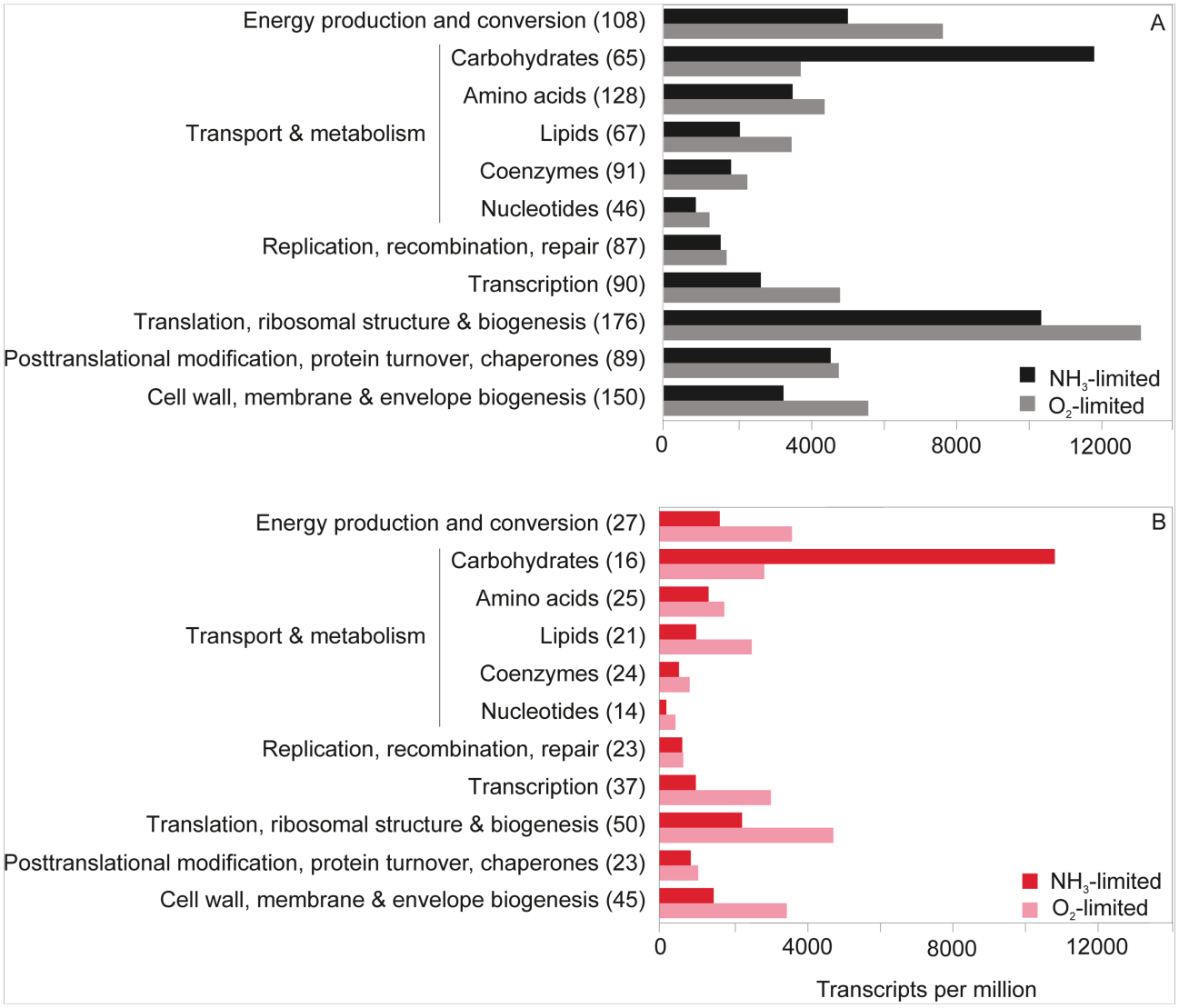

Figure 3. The sum of transcripts per million (TPM) for protein coding genes transcribed in given COG categories (number of transcribed genes per category is given in parenthesis) in the *N. europaea* transcriptomes: **A)** contribution and number of all transcribed genes in a given COG category; **B)** contribution and number of statistically significantly differentially transcribed genes in a given COG category.

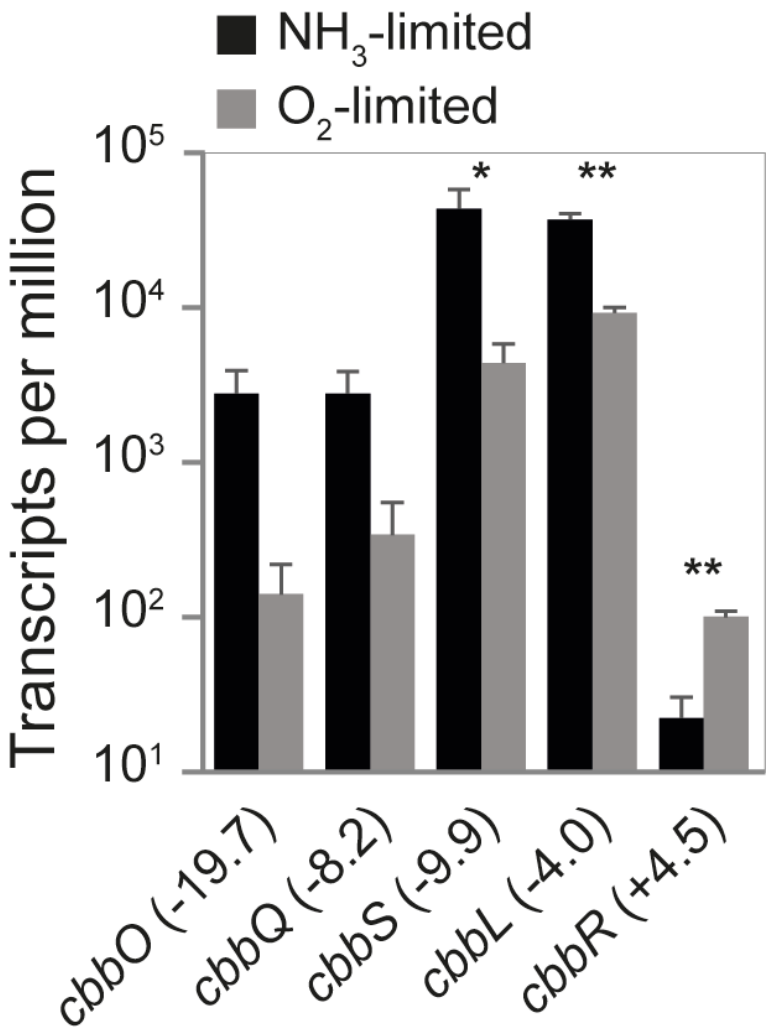

Figure 4. Mean TPM of all RuBisCO-encoding genes (*cbbOQSL*) and the corresponding transcriptional regulator (*cbbR*) in *N. europaea*. The fold change of gene transcription between NH_3- versus O_2-limited growth is given in parenthesis. Error bars represent the standard deviation between replicate samples (n=3) for each growth condition. A Welch's t-test was used to determine significantly differentially transcribed genes (* $p < 0.05$; ** $p < 0.01$). For gene annotations refer to Table S2.

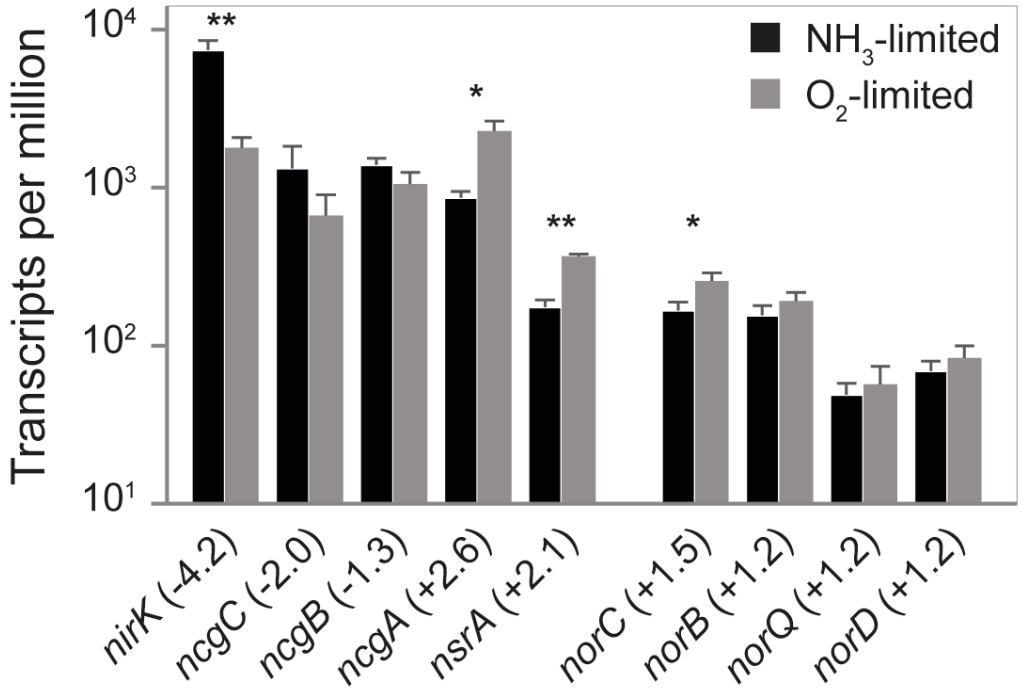

699

700 **Figure 5.** Mean TPMs of genes encoding the NirK and cNOR gene clusters in *N. europaea*. The fold
701 change of gene transcription between NH_3- versus O_2-limited growth is given in parenthesis. Error bars
702 represent the standard deviation between replicate samples (n=3) for each growth condition. A Welch's
703 t-test was used to determine significantly differentially transcribed genes (* p <0.05; ** p <0.01). For
704 gene annotations refer to Table S2.

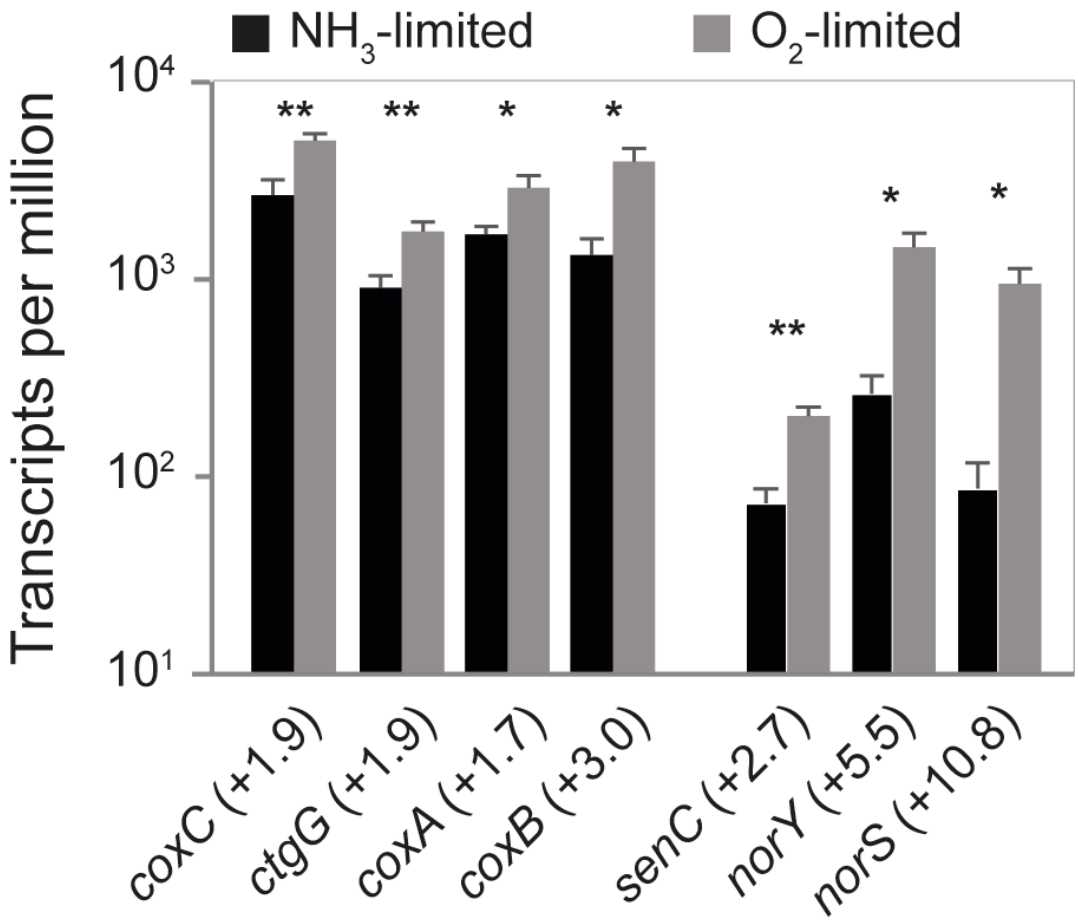

705

706 **Figure 6.** Mean TPMs of all genes encoding the A1-type and B-type HCO in *N. europaea*. The fold
707 change of gene transcription between NH_3- versus O_2-limited growth is given in parenthesis. Error bars
708 represent the standard deviation between replicate samples (n=3) for each growth condition. A Welch's
709 t-test was used to determine significantly differentially transcribed genes (* $p < 0.05$; ** $p < 0.01$). For
710 gene annotations refer to Table S2.

711